SMOOTH AND SHARP-BOUNDARY INVERSION OF TWO-DIMENSIONAL PSEUDOSECTION DATA IN PRESENCE OF A DECREASE IN RESISTIVITY WITH DEPTH

ABEL I. OLAYINKA* and UGUR YARAMANCI

Department of Applied Geophysics, Technical University Berlin, Ackerstr. 71-76, D-13355 Berlin, Germany.
** Present address: Department of Geology, University of Ibadan, Ibadan, Nigeria.*

(Received September, 2000; revised version accepted November, 2001)

ABSTRACT

Olayinka, A.I. and Yaramanci, U., 2002. Smooth and sharp-boundary inversion of two-dimensional pseudosection data in presence of a decrease in resistivity with depth. *European Journal of Environmental and Engineering Geophysics*, 7: 139-165.

The smooth and sharp-boundary inversion of two-dimensional (2D) apparent resistivity pseudosection data in cases where the half-space has a lower resistivity than the overburden is investigated. The study entailed calculation (by forward modelling) of the synthetic data over simple 2D geologic models and inversion of the data. The 2D structures modelled include vertical fault, graben and horst. The Wenner array was used.

The results show that there is generally an improvement in the model misfit with iteration number in smooth inversion; the algorithm can then be expected to iterate to the best solution at a high iteration number where the model resistivity of the substratum approaches the true bedrock resistivity. Inversion of the data using sharp boundaries indicates that the range of 2D equivalence, for which a reasonable interpretation could be attained, is relatively narrow. For the equivalent solutions, the data misfit between the observed and the calculated data is very small while model interpretations that are wrong can be readily identified on account of very large data misfits.

A field example is given from Nauen, northern Germany, where partly-saturated sand of high resistivity is underlain in succession by less resistive saturated sand and glacial till; the smooth and sharp-boundary inversion results are in good agreement with the geo-radar and surface magnetic nuclear resonance (SNMR) and borehole information.

KEY WORDS : apparent resistivity pseudosection data, smooth inversion, sharp-boundary inversion, Wenner array, northern Germany.

1359-8155/02/$5.00

INTRODUCTION

Commercially available software can now be routinely employed for inversion of 2D apparent resistivity data. These inversion programs can be classified into two groups, namely smooth inversion and sharp boundary (block) inversion. Smooth inversion is a cell-based inversion while in block inversion polygons are employed to define layers and/or bodies of equal resistivity. Olayinka and Yaramanci (1999, 2000a,b) have reported the ability of these inversion schemes in defining the geometry and true resistivity of subsurface structures, in the case where the resistivity increases with depth. Situations may, however, also arise in environmental, engineering and hydrogeologic investigations in which there is a decrease in resistivity with depth. The present work, has consequently, examined the inversion schemes in situations in which there is a decrease in resistivity with depth. Synthetic data over 2D geologic models such as vertical fault, graben and horst were considered.

An example of a smooth 2D inversion algorithm is RES2DINV by Loke and Barker (1996) while the program RESIX IP2DI by Interpex (1996) is representative of a block inversion scheme. While the program RES2DINV is fully automatic, RESIX IP2DI requires that the interpreter prescribe an initial geological model as part of the input. It is demonstrated in this work that such a starting model could be based on a plane layer earth model. This simple approach has the added advantage that only the depth to the interface(s) need be varied as the inversion result is, for all practical purposes, not dependent on the resistivity contrast in the starting model. As the depth to interface in the starting model is increased, it is shown that, contrary to what would be expected intuitively, there is no smooth progression in the inverted model. In other words, it is possible to obtain a reasonable interpretation for both shallow and large depths to the bedrock interface in the starting model. Fortunately, the data rms misfit between the calculated and the synthetic 'observed' data is very diagnostic in identifying a reasonable interpretation. The bad inverted models are invariably attained after very few iterations and accompanied by a high data misfit. On the other hand, the good models are attained after several iterations, with much lower data misfit. With this interpretation procedure, it is shown that the range of 2D equivalence is very narrow for the case in which there is a decrease in resistivity with depth.

A test with data was also conducted from a field example from Nauen, northern Germany, to demonstrate the usefulness of the two inversion schemes in interpreting real data.

OUTLINE OF THE PROCEDURE

Forward modelling of apparent resistivity pseudosection data

A 2D forward modelling program, RESIX IP2DI generated the apparent resistivity pseudosection data, by Interpex (1996). The program uses a finite element approach to solve for the potential distribution due to point sources of current, and the potential distribution is converted into apparent resistivity values. The modelling routine accounts for 3D sources (current electrodes) in a 2D material model. This implies that the resistivity can vary arbitrarily along the line of surveying (x-direction) and with depth (z-direction), but the models have an infinite perpendicular extension along the strike (y-direction). In all cases of the synthetic data, a layout with 81 electrodes was modelled with the Wenner array. The X- and Z- spacings are normalised with respect to the minimum electrode spacing A. In order to reduce the number of model parameters to be considered, the theoretical data have been limited to a single resistivity contrast of 20:1 between the overburden and the bedrock. Tests with several models indicate that the forward modelling program does not contain any systematic error. Moreover, the results are in agreement with those from another program RES2DMOD (Loke and Barker, 1996) which uses a finite difference method for the forward modelling.

Gauss distributed random noise with a standard deviation of 5% was added to the calculated responses for all the models in order to simulate field conditions. The synthetic apparent resistivity data were then inverted using a smooth and a block inversion scheme, respectively.

Smooth inversion

The program RES2DINV (Loke and Barker, 1996) was employed for the smooth inversion. A forward modelling subroutine is used to calculate the apparent resistivity values, and a non-linear least-squares optimisation technique is used for the inversion routine (DeGroot-Hedlin and Constable, 1990; Loke and Barker, 1996; Dahlin and Loke, 1998). The 2D model used by the inversion program consists of a number of rectangular blocks whose arrangement is loosely tied to the distribution of the datum points in the pseudosection. The distribution and size of the blocks are automatically generated by the program so that the number of blocks do not exceed the number of datum points.

The inversion routine uses the Gauss-Newton method for a smoothness-constrained least-squares inversion, for which by default the vertical and horizontal smoothness constrains are the same (DeGroot-Hedlin and

Constable, 1990). The smoothness constrain increases with 10% per layer, which, along with increasing layer thickness, reduces the resolution with depth. The inversion is based on an analytical calculation of the sensitivity matrix (Jacobian matrix) for a homogeneous halfspace and the sensitivity matrix is re-calculated using the finite element method at each step of the iteration. The optimisation equation (Ellis and Oldenburg, 1994) can be represented as:

$$(\mathbf{J}_i^T\mathbf{J}_i + \lambda_i\mathbf{C}^T\mathbf{C})\mathbf{p}_i = \mathbf{J}_i^T\mathbf{g}_i - \lambda_i\mathbf{C}^T\mathbf{C}\mathbf{r}_{i-1} \quad , \tag{1}$$

where $\mathbf{J}_i$ is the Jacobian matrix of partial derivatives, $\mathbf{J}_i^T$ represents the transpose of $\mathbf{J}_i$, $\mathbf{g}_i$ is the discrepancy vector which contains the difference between the logarithms of calculated and observed apparent resistivity values, $\mathbf{p}_i$ is the perturbation vector to the model parameters, λ_i is a damping factor (or Lagrange multiplier) used to reduce the amplitude of $\mathbf{p}_i$, $\mathbf{C}$ is a flatness-filter matrix used to minimise the roughness of $\mathbf{p}_i$. The second term on the right-hand side of equation (1) applies the smoothness constraint directly on the model resistivity vector, $\mathbf{r}_{i-1}$. This guarantees that the model will be smooth subject to the damping factor used (Ellis and Oldenburg, 1994). It also reduces the oscillations in the model resistivity values.

Block inversion

The interactive program RESIX IP2DI by Interpex (1996) was employed for the block inversion. This is a finite element forward and inverse modelling program that calculates the resistivity responses of 2D earth models (Rijo, 1977; Petrick et al., 1977; Pelton et al., 1978). A finite element mesh is generated; each rectangular element is divided into 4 triangles and the resistivity of each triangle under the electrode spread is defined from the properties of the polygons which make up the model. The program uses ridge regression inversion (Inman, 1985) of polygon-based 2D models to best fit the 2D pseudosection data in a least squares sense.

With the aid of a mouse and using an interactive graphics screen, it is required that the interpreter creates a 2D model defined by the vertices (i.e., the corners). The polygons can be constructed as a combination of up to 100 bodies and layers and up to 1000 vertices per model. Moreover, groups of vertices can be locked together to form a single unit whose x- and/or z-position can be used as an inversion parameter. The inversion is used to automatically improve the fit of the model by (automatically) adjusting some model parameters. As part of the inversion procedure, the body resistivity and position of vertices are allowed to change in the calculation and the user is able to specify which parameters to vary and which parameters to freeze. The finite element grid is determined from the number of electrodes and the electrode spacing. The program automatically creates a fine grid, which can be edited using the mouse. Vertical and horizontal

elements can be inserted or deleted and elements can be split in half using the mouse.

The inverted parameters are given by:

$$\mathbf{P} = (\mathbf{G}^T\mathbf{G} + k\mathbf{I})^{-1}\,\mathbf{G}^T\,\mathbf{F}_h \quad , \tag{2}$$

for a weighted matrix **G** containing the derivatives of each data point with respect to each model parameter; T denotes transpose, **I** is the identity matrix; $\mathbf{F}_h$ is the data vector. The matrix **G** is overdetermined as there are more data than parameters. The $\mathbf{G}^T\mathbf{G}$ is square, symmetric and positive definite. k is a small positive constant which is added to the diagonal terms of the $\mathbf{G}^T\mathbf{G}$ before inversion and has the effect of damping the small eigenvalues of $\mathbf{G}^T\mathbf{G}$ which otherwise cause instability, while at the same time it has minor effect on the larger eigenvalues associated with the more well-determined parameters. Several values of k on a logarithmic scale are tried while iterating towards a solution, in order to minimise the least-squares residual. If the vector **e** is defined as $\mathbf{F}_h - \mathbf{F}_t$ (i.e., the difference between the measured data $\mathbf{F}_h$ and the model data $\mathbf{F}_t$), the residual sum of squares for the ridge regression solution is given by:

$$S = (\mathbf{e})^T\,\mathbf{e} \quad . \tag{3}$$

Marquardt's (1963) algorithm determines the smallest value of k for which the ridge regression estimator of equation (2) will yield a new model that better fits the field data. As the inversion process nears a solution or a minimum in the residual sum of squares (equation 3), successively smaller values of k are used.

Trial tests with several synthetic data have shown that the initial model for the block inversion can be based on a simple horizontal layer model. Several examples of these are presented in the following section. The effects of both the depths to the bedrock interface and the layer resistivities in the initial model on the inversion results are described. The model parameters used in this work are given in Table 1.

Table 1. Definition of model parameters used in this work.

A :	minimum electrode spacing
Z :	depth
$H_{(initial)}$:	depth to the bedrock interface in the two-layer model used as starting model for block inversion
$\rho_{n(true)}$:	the true resistivity of the n-th layer
$\rho_{n(initial)}$:	the prescribed resistivity of the n-th layer for the initial model.
$\rho_{n(model)}$:	the resistivity of the n-th layer after the data rms misfit has converged in block inversion

THEORETICAL EXAMPLES

The model responses of some idealized 2-dimensional structures of geological relevance were calculated using the 2D finite element forward modelling program. The calculated model responses, with 5% Gaussian noise added, were used as input for the 2D inversion routines. Calculation of the data misfit involves a comparison, for the respective datum points, between the observed apparent resistivities ($\rho_{a\,(obs)}$) and the calculated values ($\rho_{a\,(calc)}$), as:

$$D_i = [(\rho_{a\,(obs)} - \rho_{a\,(calc)})/\rho_{a\,(obs)}] \cdot 100\% \quad . \tag{4}$$

For the entire pseudosection the data rms misfit, D_{rms}, is given, as

$$D_{rms} = [(1/N)\ \Sigma\ D_i^2]^{1/2} \quad . \tag{5}$$

The convergence criterion used in the block inversion was the change in the data rms error defined as

$$d_j = (D_{rms,j} - D_{rms,j+1})/D_{rms,j+1} \quad , \tag{6}$$

where $D_{rms,j}$ and $D_{rms,j+1}$ are the rms errors for the j-th and (j+1)-th iterations. The inversion process is terminated when d_j is less than 3%. In the discussion that follows, the normalised D_{rms} is the data rms misfit in the inverted model divided by 5%, the latter being the amount of Gaussian noise in the synthetic data. A model rms misfit M_{rms} could similarly be calculated from a comparison of the inverted model in the smooth inversion with the known theoretical 2D model.

Vertical fault

An example to illustrate the inversion of apparent resistivity data over a vertical fault is presented in Fig. 1. The depth to the top of the fault is 1A and the fault throw is 4A, where A is the minimum Wenner electrode spacing. The resistivity of the overburden is 2000 Ωm while that of the half-space is 100 Ωm. Gaussian noise with amplitude of 5% was added. The apparent resistivity data set was inverted, first with the smooth inversion program (RES2DINV) and next with the block inversion program (RESIX IP2DI).

The apparent resistivity pseudosection data (Fig. 1a) range between about 91 and 2259 Ωm; there is a decrease in the apparent resistivities with the electrode spacing. Moreover, there is a steepening of the contours at about the centre of the line. The models obtained at various iteration steps in the smooth inversion of this data set are shown in the left-hand panels of Fig. 2 while the

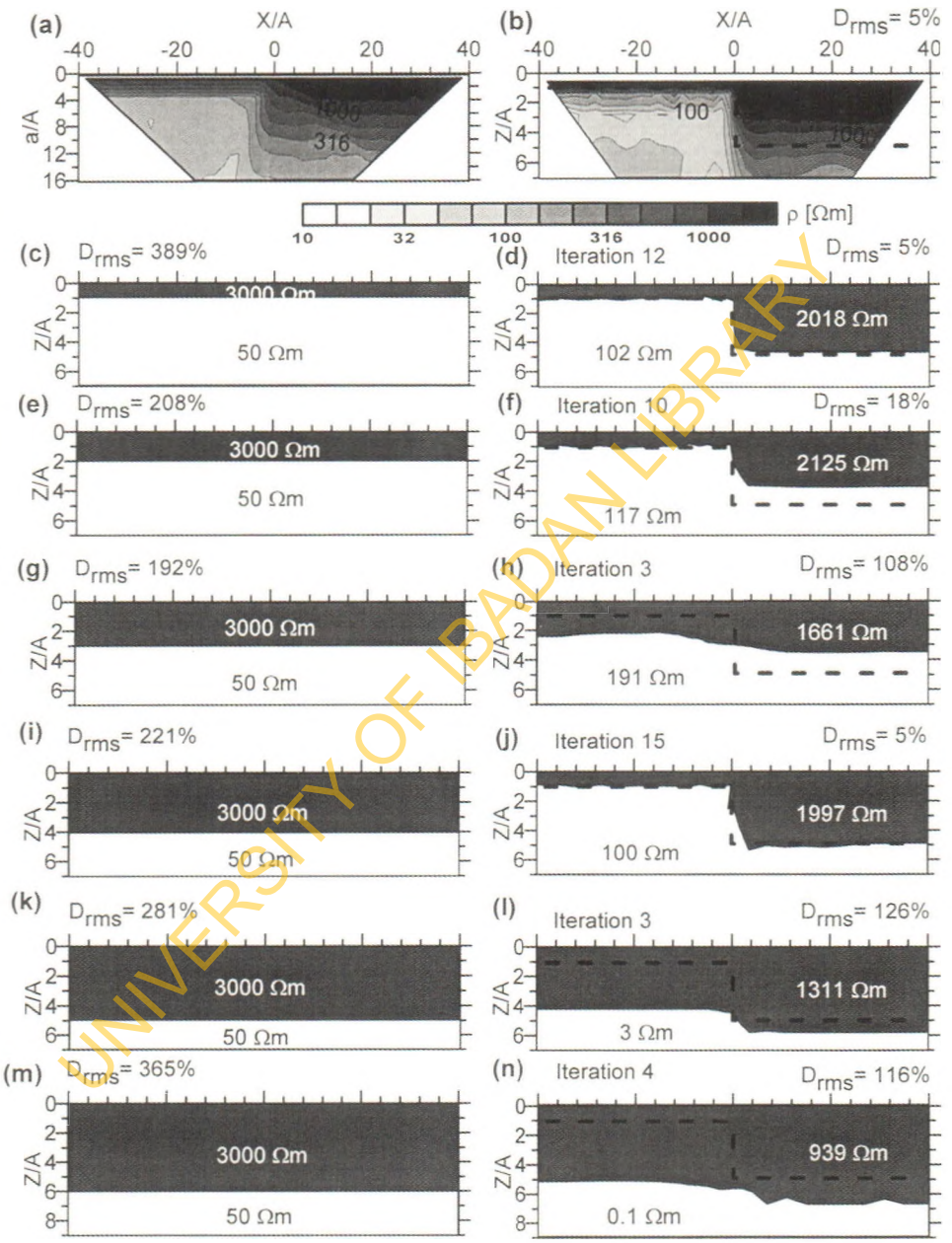

Fig. 1. Interpretation of data over a vertical fault model. (a) Synthetic apparent resistivity pseudosection data containing 5% Gaussian noise. (b) Model obtained from smooth inversion. From (c) to (n), the left-hand panels are the initial models for sharp-boundary algorithm while the right-hand panels are the corresponding inverted models. The outline of the true structure is shown as a dashed line. A is the minimum Wenner spacing.

corresponding model misfits are presented in the right-hand panels. There is an improvement in the model rms misfit for successive iterations. For the fourth iteration, the model resistivities vary between about 43 and 4019 Ωm. Over the overburden, the model resistivities range between about 322 and 4019 Ωm. On the other hand the model resistivities over the substratum range between about 43 to 516 Ωm. The problem of defining the position of the contact, however, remains.

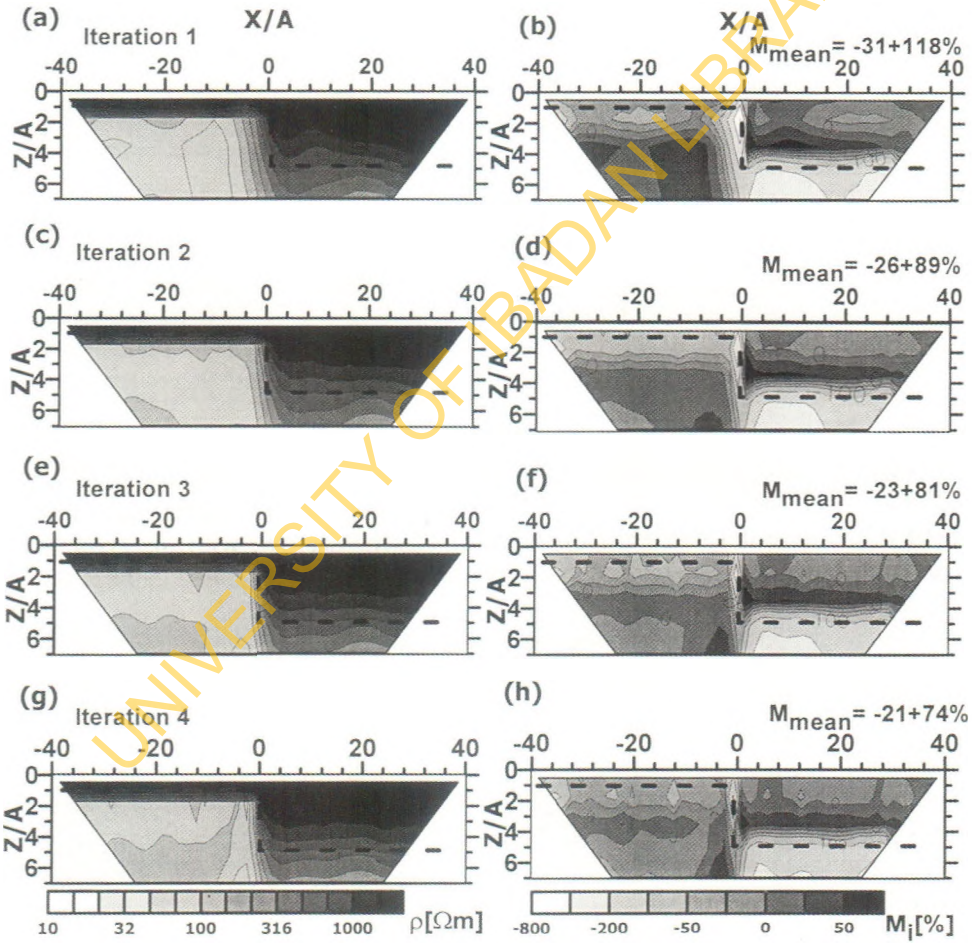

Fig. 2. Inverted model (the left-hand panels) at various iteration steps in the smooth inversion of the data in Fig. 1a and the corresponding model misfit (the right-hand panels).

A 2-layer model with a horizontal interface was employed as the initial model for the block inversion of the data. The resistivity of the upper layer is 3000 Ωm while that of the substratum is 50 Ωm. The depth to the bedrock interface ($H_{initial}$) was varied from 1A to 6A. The corresponding inverted models are shown in the left-hand panels from Figs. 1d to 1n. It should be noted that, contrary to what would be expected intuitively, there is no smooth progression in the respective models, in terms of the D_{rms}, the number of iteration required before convergence was achieved and the depth to the bedrock interface in the downthrown block. The D_{rms} indicates an increase from ($H_{initial}$) = 1A to ($H_{initial}$) = 3A; there is another minimum for ($H_{initial}$) = 4A, beyond which the D_{rms} diverges. The relationship is somewhat complicated and this can be partly explained from the 2D nature of the true model and the fact that the inversion is a non-linear problem.

The inverted models indicate that a reasonable (equivalent) interpretation was possible only for ($H_{initial}$) = 1A and ($H_{initial}$) = 4A. In these two cases, the data rms misfit converged, albeit slowly, over several iterations. For these inverted models $\rho_{1(inverted)} \approx \rho_{1(true)}$ and $\rho_{2(inverted)} \approx \rho_{2(true)}$ (Fig. 2). The inverted model for ($H_{initial}$) = 2A (Fig. 1f) can still be regarded as a reasonable interpretation, although there is a depth underestimation in the downthrown block. The D_{rms} in this model is intermediate, while convergence was achieved after several iterations during the block inversion. On the other hand, the D_{rms} converged rapidly (after very few iterations) to a very high level with the other initial models, and it was difficult to obtain a reasonable interpretation in those instances. The range of equivalent models, for which the normalised data rms misfit in the inverted models approaches 1, is very narrow, with the error in estimating the overburden and bedrock resistivities being very negligible. Moreover, the position of the vertical contact is accurately delineated. Fig. 3 shows that there is, in general, a linear correlation between the D_{rms} and the error in layer resistivities for the 2D models obtained from the sharp boundary inversion. This indicates that the D_{rms} is a good measure of the reasonableness (or otherwise) of the inverted model.

It may be noted that the starting D_{rms} is not necessarily a very useful guide to the possibility of attaining a good inverted model. For example, comparing Figs. 1c and 1g, while the initial D_{rms} in the former was very high at 389%, it was still possible to obtain a reasonable interpretation after several iterations. On the other hand, although the starting D_{rms} in Fig. 1g was relatively low at 192%, it was very difficult to attain a good fit as the D_{rms} converged after a few iterations to a high level. Most of the results obtained from the inversion of the fault model are applicable to a large extent to the other synthetic data tested as discussed below.

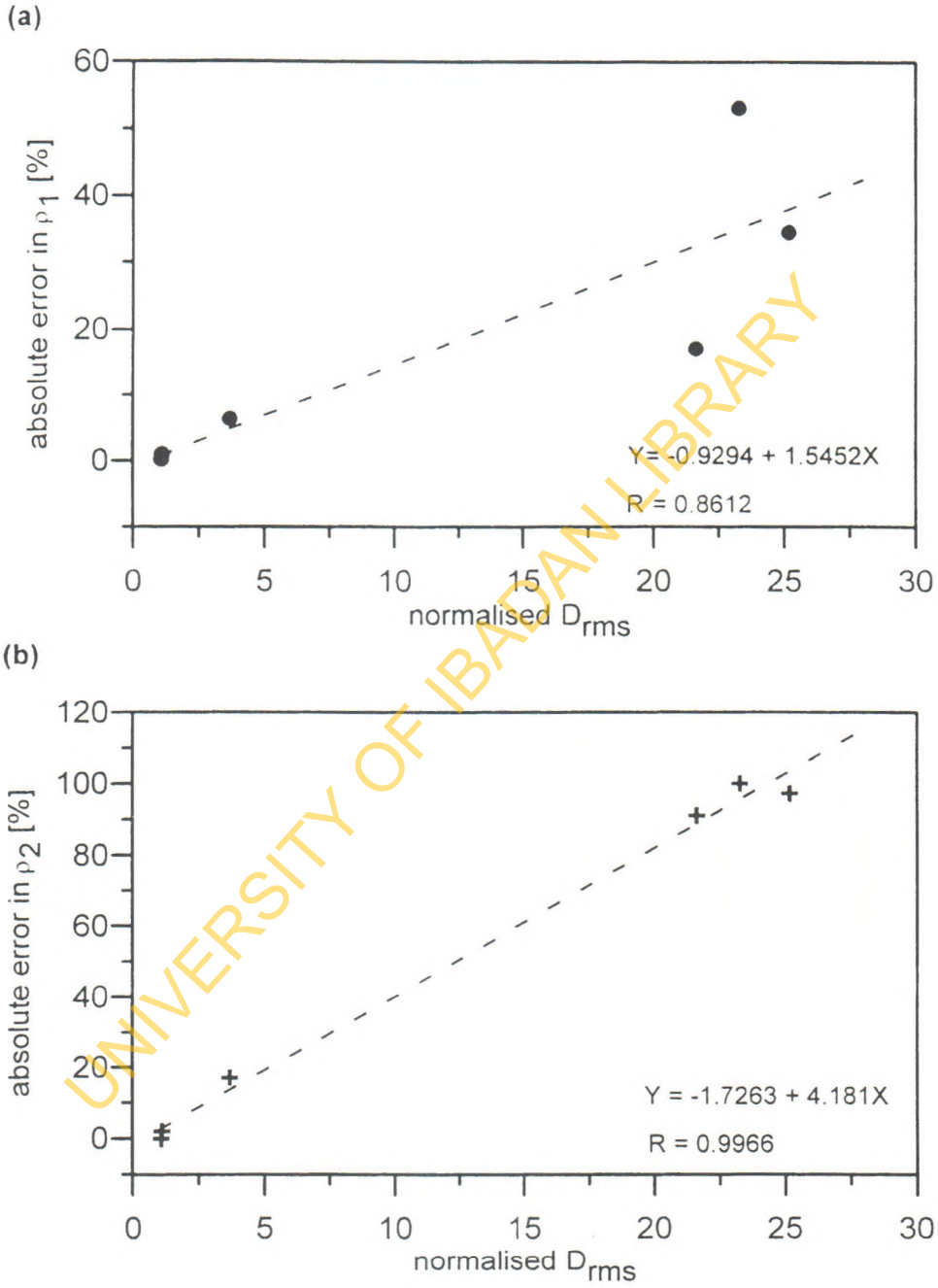

Fig. 3. Correlation between the data rms misfit and the error in layer resistivities for the 2D models obtained from the sharp boundary inversion of the data in Fig. 1. (a) Resistivity of the overburden. (b) Resistivity of the substratum.

Horst model

The apparent resistivity pseudosection data shown in Fig. 4a was calculated from a horst structure where the model parameters include a depth to top of 1A, depth to base is 5A, the width is 8A while the resistivity contrast between the overburden and the substratum is 20:1. The resistivities range between about 132 and 2227 Ωm. The data rms misfit converged at the fourth iteration with the smooth inversion algorithm and the inverted models are presented in Fig. 5. The model resistivities over the overburden range between about 272 and 4108 Ωm. For the substratum, the model resistivities range between about 21 and 542 Ωm. It may be noted that there is a decrease in the model rms misfit for successive iteration steps.

A 2-layer model in which the upper layer has a resistivity of 3000 Ωm while the bedrock has a resistivity of 50 Ωm was employed as the starting model for the sharp-boundary inversion algorithm. Six trials were made, in which the depth to the bedrock interface was varied from 1A to 6A, respectively. The starting models are presented in the left-hand panels of Fig. 4 (i.e., c to m), while the corresponding inverted models are shown in the right-hand panels (Figs. 4d to 4n). Equivalent 2D models, with low data rms misfits, were obtained only in two instances, namely those in which $H_{(initial)}$ = 1A and $H_{(initial)}$ = 3A; in these instances, convergence of the D_{rms} was achieved only after a large number of iteration steps in the inversion. In these inverted models, the error in the estimate of the both the overburden and bedrock resistivities are low. Moreover, the position of the horst structure is accurately delineated. It was not possible to attain a reasonable interpretation of the apparent resistivity data with the other four initial models, as indicated by the very high data rms misfit which was attained at relatively low iteration numbers. In these cases, only little changes in the bedrock configuration was recorded from the initial model (with a planar interface) and the inverted model. A comparison between the inverted model in Fig. 4f and its starting model shows that there has been little or no change to the bedrock interface; rather the major changes are with respect to the resistivities. There is a linear relationship between the D_{rms} for the best fit models from the sharp boundary inversion and the errors in estimating the layer resistivities (Fig. 6).

Trough model

The apparent resistivity pseudosection data presented in Fig. 7a was calculated over a trough structure in which the depth to the top is 1A while the depth to the base is 5A. The width of the structure is 8A while the resistivity contrast between the overburden and the bedrock is 20:1. The apparent resistivities range between 67 and 1982 Ωm. During the smooth inversion of the data, the data rms misfit converged at the end of the fourth iteration (Fig. 8).

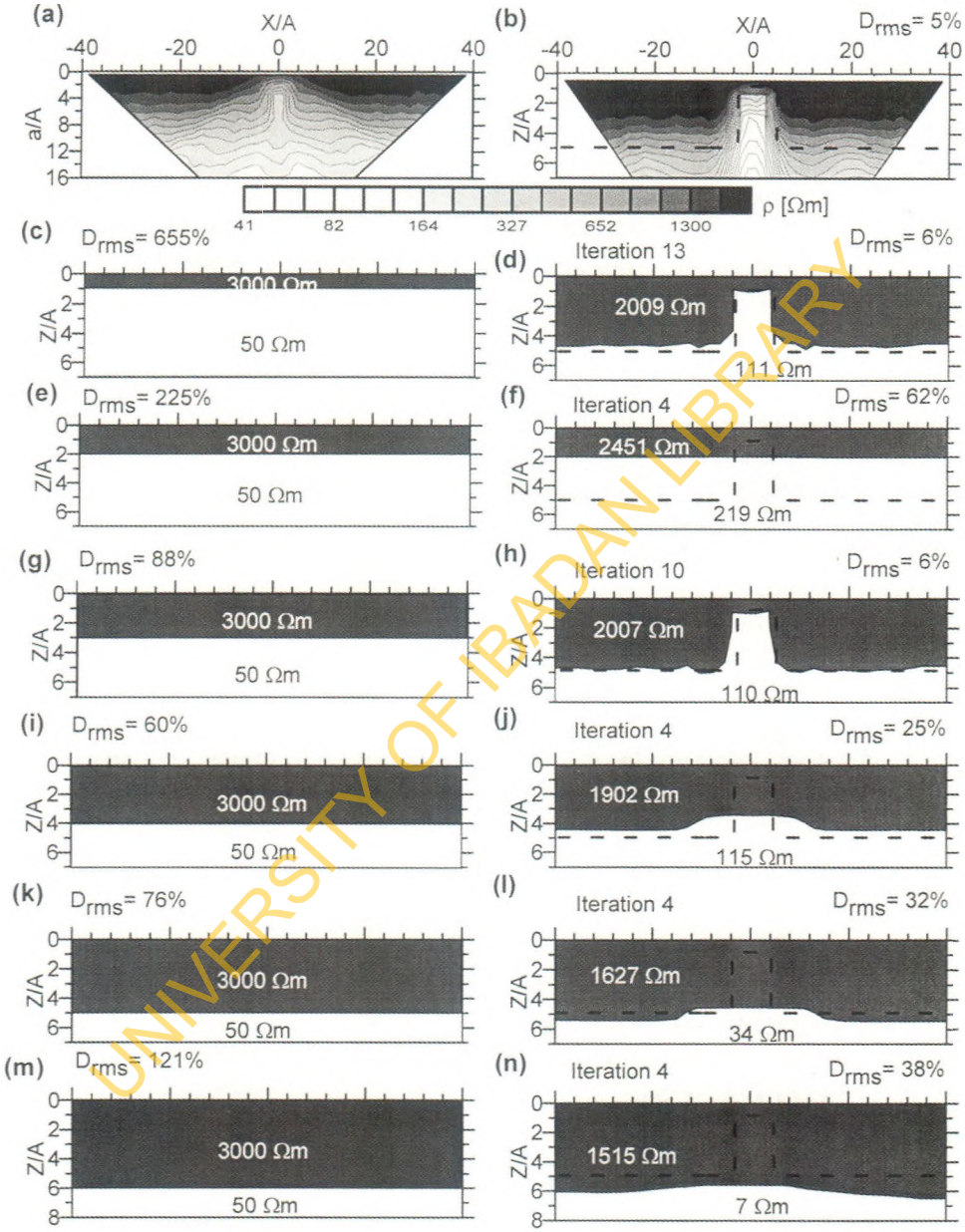

Fig. 4. Example of the inversion of data over a horst structure. The width is 8A, the depth to the top 1A and the depth to the base 5A. The resistivity contrast is a factor of 20. (a) Synthetic pseudosection data containing 5% Gaussian noise. (b) Inverted model obtained from smooth inversion at iteration 4. From (c) to (n), the left-hand panels are the initial model for sharp-boundary algorithm while the right-hand panels are the corresponding inverted model.

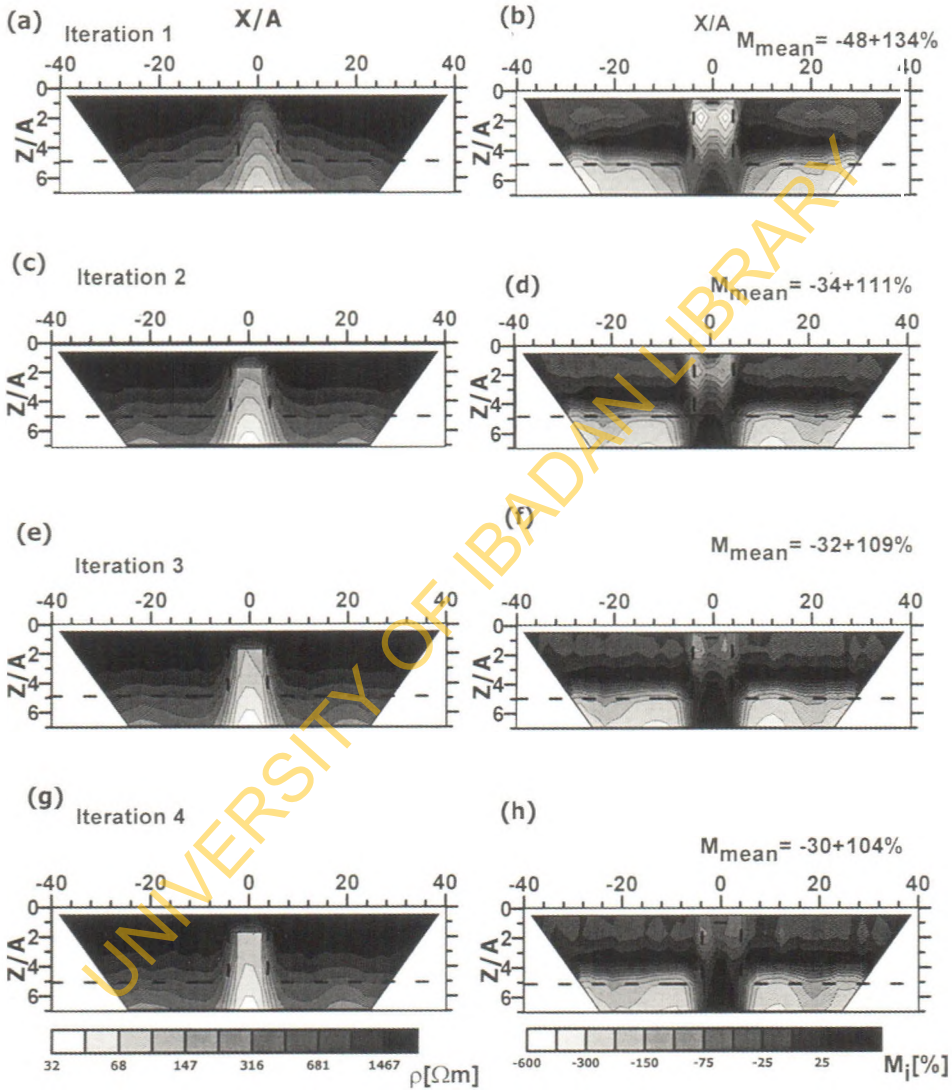

Fig. 5. Inverted model (the left-hand panels) at various iteration steps in the smooth inversion of the data in Fig. 4a and the corresponding model misfit (the right-hand panels).

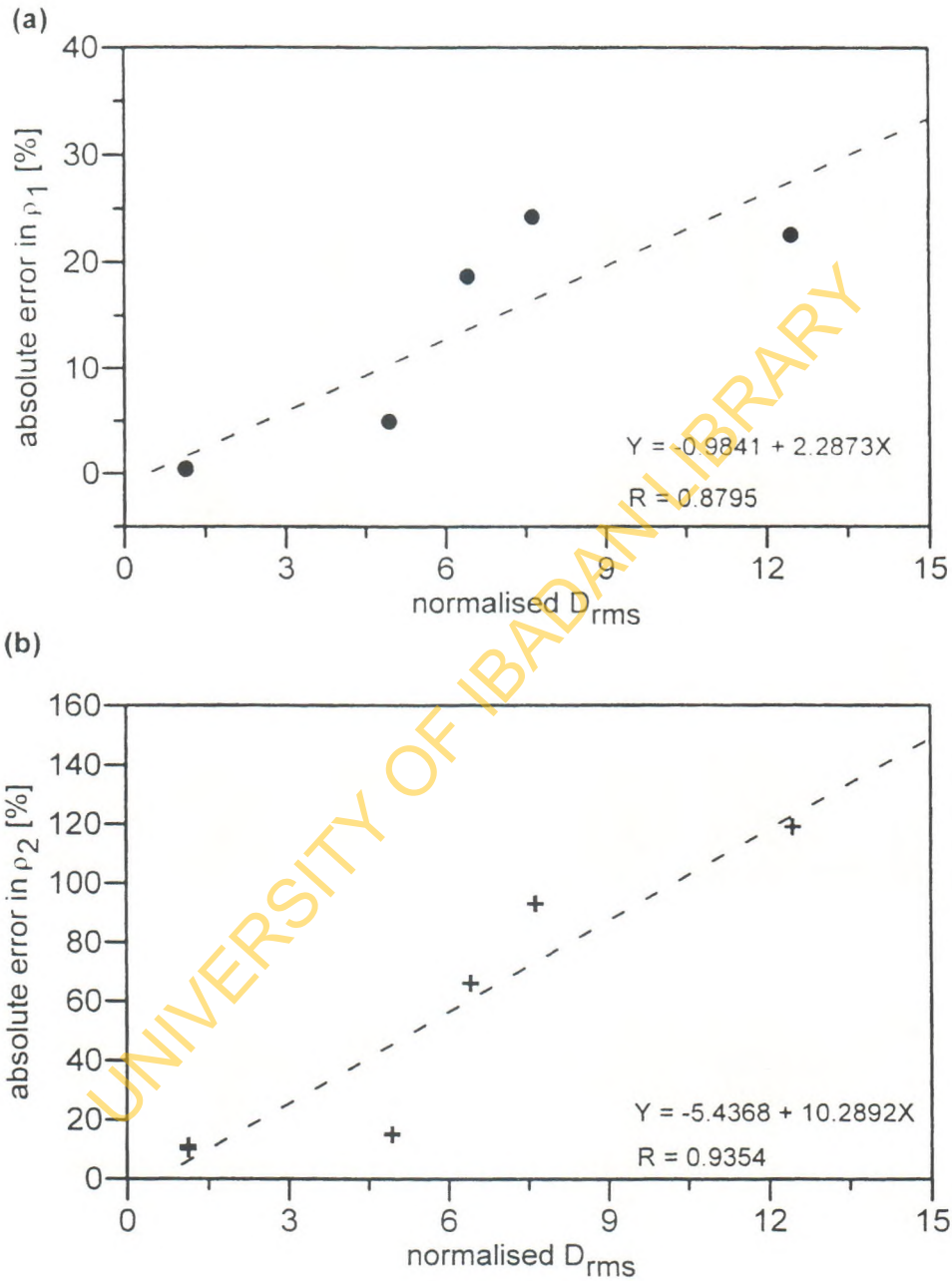

Fig. 6. Correlation between the data misfit and the error in layer resistivities for the equivalent 2D models in the sharp boundary inversion in Fig. 5. (a) Resistivity of the overburden. (b) Resistivity of the substratum.

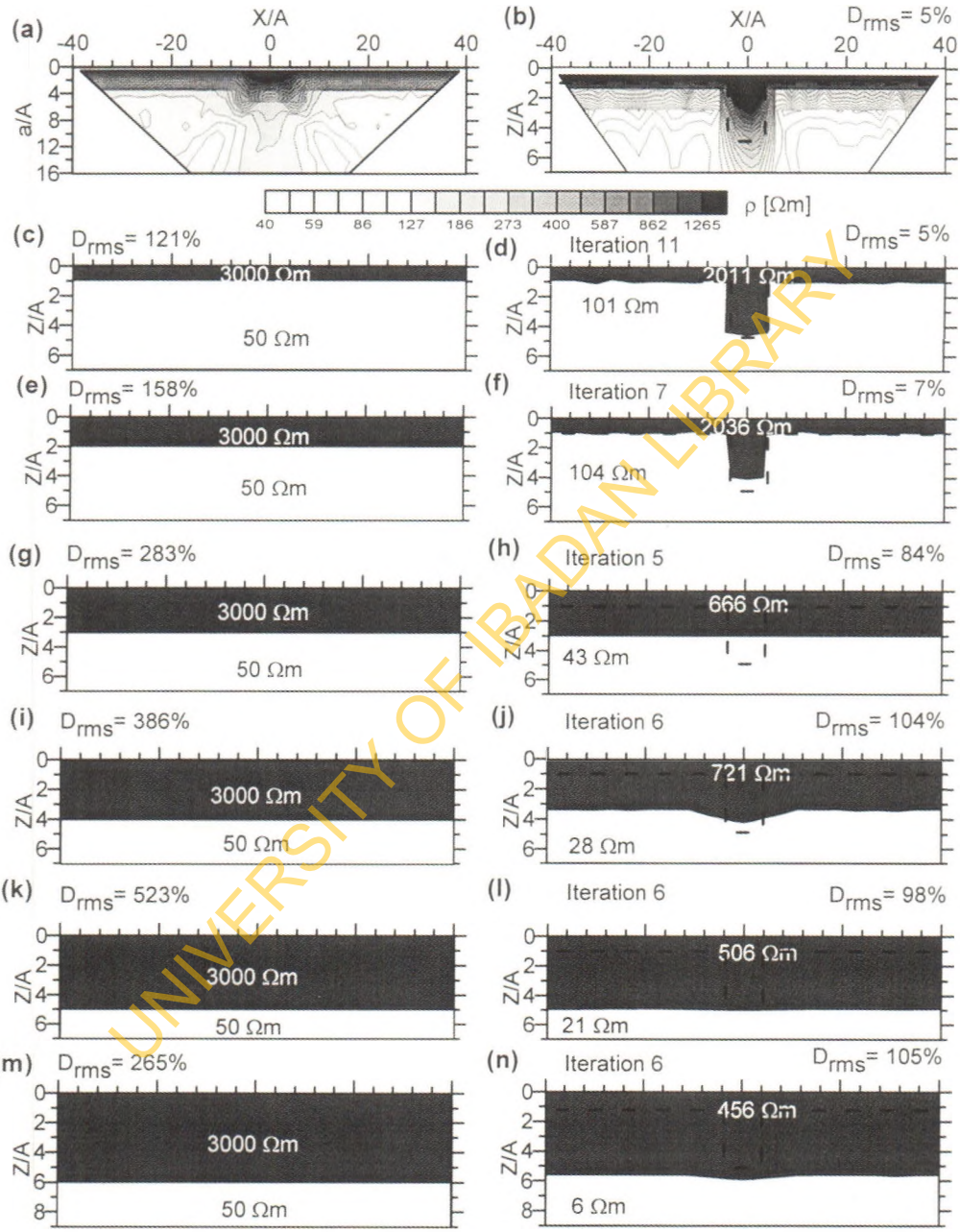

Fig. 7. Interpretation of pseudosection data over a trough model. (a) Synthetic data containing 5% Gaussian noise. (b) Model obtained from smooth inversion. From (c) to (n), the left-hand panels are the initial model for sharp-boundary algorithm while the right-hand panels are the corresponding inverted model.

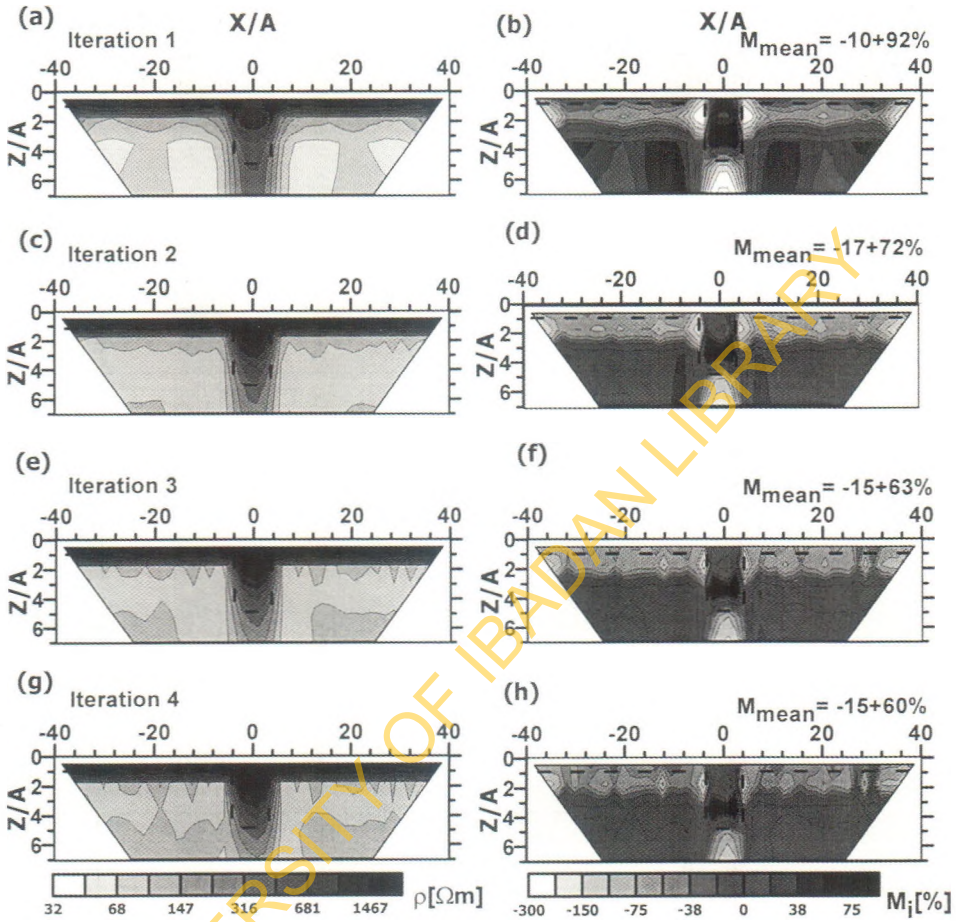

Fig. 8. Inverted model (the left-hand panels) at various iteration steps in the smooth inversion of the data in Fig. 7a and the corresponding model misfit (the right-hand panels).

There is a high resistivity anomaly centred around the position of the trough structure although it is not possible to locate the bottom of the anomaly. Over the overburden, the model resistivities vary between about 237 and 3732 Ωm. On the other hand, the model resistivities within the substratum vary between about 58 and 529 Ωm.

A 2-layer model in which the resistivity of the upper layer is 3000 Ωm while that of the half-space is 50 Ωm, was used as the starting model for the sharp-boundary inversion algorithm. The depth to the bedrock interface was

varied from 1A to 6A. The results indicate that reasonable (equivalent) interpretations were possible for $H_{(initial)}$ = 1A and $H_{(initial)}$ = 2A. In these two inverted models, the layer resistivities are accurately modelled while the limits of the trough structure are well defined. A comparison between the inverted models in the remaining cases and their starting model shows that there has been little or no change to the bedrock interface; rather the major changes are with respect to the resistivities. The data misfits for those models are consistently very high, indicating a poor fit.

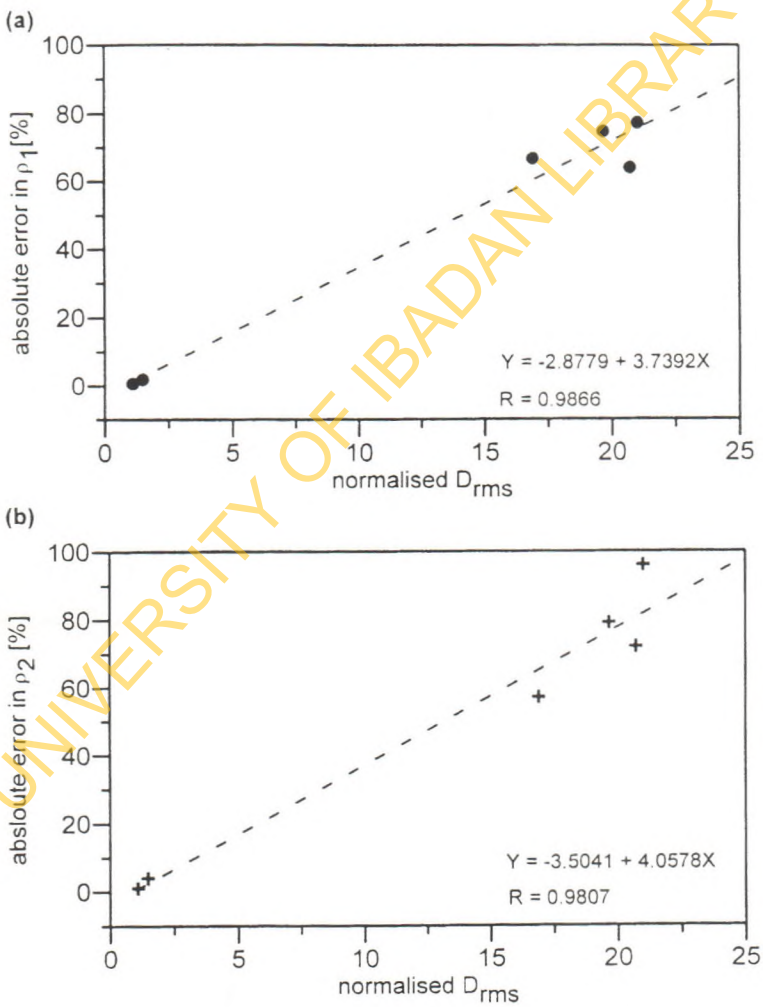

Fig. 9. Correlation between the data rms misfit and the error in layer resistivities for the best-fit 2D models in the sharp boundary inversion in Fig. 8. (a) Resistivity of the overburden. (b) Resistivity of the substratum.

As was the case with the fault and the horst structures, there is a linear relationship between the data misfit in the sharp-boundary inversion and the error in estimating the layer resistivities (Fig. 9).

Extension to two overburden units

The pseudosection data set presented in Fig. 10a was calculated from a vertical fault structure buried beneath two overburden units. The resistivity of the shallower overburden unit is 1000 Ωm and its thickness 1A. The resistivity of the lower unit is 300 Ωm. The depth to the top of the fault is 2A while the depth to its base is 5A. The resistivity of the substratum is 100 Ωm. The calculated apparent resistivities range between about 96 Ωm and 913 Ωm. As would be expected, the anomaly is somewhat suppressed, reflecting the influence of the two overburden units. During the inversion of the apparent resistivities with the smooth inversion algorithm, the data misfit converged at the end of the fourth iteration and the model obtained is shown in Fig. 10b.

A 2-layer plane layer solution in which the resistivity of the upper layer is 1500 Ωm while that of the substratum is 50 Ωm was first attempted in interpreting the data. The depth to the bedrock interface was varied from $H_{(initial)}$ = 1A to $H_{(initial)}$ = 5A. The inverted models are presented in the left-hand panels of Fig. 10c to 10l. It can be observed that in each and all the cases, the inverted model was "out-of-phase" with the data, as suggested by the high D_{rms}. None of these inverted models could, therefore, be accepted as a reasonable interpretation of the data.

To reduce the data rms misfit, a 3-layer model, in which there is a decrease in resistivity with depth, was tried. The layer resistivities are 1500, 500 and 50 Ωm, respectively. The thickness of the first layer is 1A in all the cases while the depth to the bedrock interface was progressively increased from 2A to 6A, in steps of 1A. The inversion results (Fig. 11) indicate that the data rms misfit converged to a relatively low level in all the cases. The model resistivity for the first layer ranged between 975 and 1049 Ωm. This is in good agreement with the true value of 1000 Ωm. The resistivity of the intermediate layer ranged between 228 and 342 Ωm which is close to the true value of 300 Ωm. Similarly, the bedrock model resistivity ranges between about 86 and 103 Ωm which is in good agreement with the true value of 100 Ωm. While the thickness of the shallowest layer is accurately imaged in all the cases, there is a progressive increase in the depth to the downthrown block in the inverted model as $H_{(initial)}$ increased. On account of the low D_{rms}, any of these inverted models could be taken as a reasonable (equivalent interpretation) of the data.

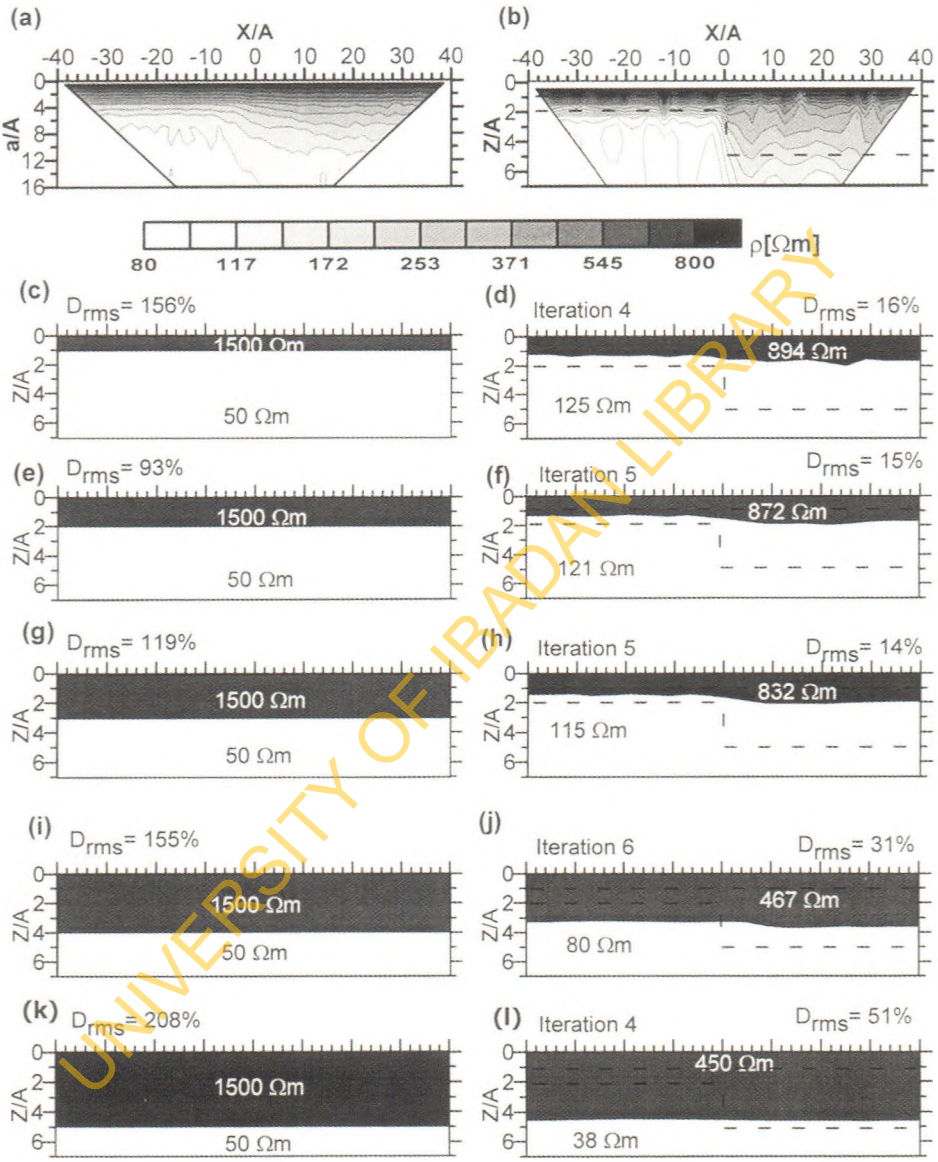

Fig. 10. Interpretation of data over a vertical fault model in which there are two overburden units. (a) Synthetic data containing 5% Gaussian noise. (b) Model obtained from smooth inversion. From (c) to (l), the left-hand panels are the initial model for sharp-boundary algorithm while the right-hand panels are the corresponding inverted model. Note that only one overburden unit was prescribed for the sharp boundary inversion.

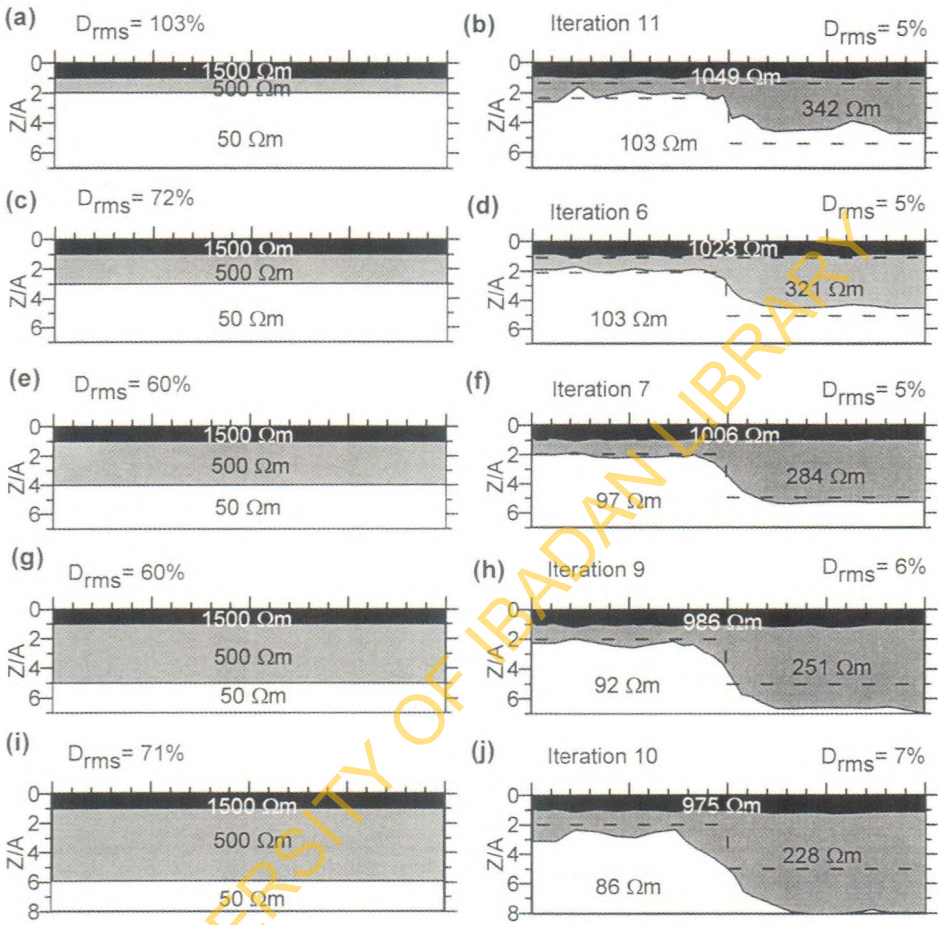

Fig. 11. Re-interpretation of data over the vertical fault model in Fig. 10. The left-hand panels are the initial model for sharp-boundary algorithm while the right-hand panels are the corresponding inverted model. Two overburden units were prescribed in the initial models.

FIELD EXAMPLE

In this section, field data measured as part of an integrated hydrogeological and geophysical survey at Nauen, northern Germany (Fig. 12), is described to illustrate the application of the interpretation procedure presented above when dealing with real data. The surface geology in this area dates from the last glacial epoch. The hills are underlain by till while the low ground

comprises glaciofluvial sands and gravels. There is an unconfined shallow aquifer consisting of fine to medium sand with a porosity of between 30 to 35% (Yaramanci et al., 1999). It is underlain by an aquiclude of marly and clayey glacial till. The glacial till certainly has a high porosity, may be around 20 to 30%, although this is not known precisely. As it comprises fine-grained material, most of the water is adsorbed and only a small part is free; hence the low effective porosity of approximately 5%. The glacial outcrops north of the site with an almost W-E strike; for this reason, all the measurement profiles were chosen N-S. The electrode spacing was 2 m while the entire line is 256 m long.

The measured data range between about 37 and 4733 Ωm (Fig. 13a). There is a decrease in the apparent resistivity at larger spacings and the presence of a near-surface material of high resistivity towards the southern end of the line is indicated. This material is probably absent towards the northern end. There is a steepening of the contours between a distance of about X = 160 to 170 m along the line. Most of the features observed from the measured data are also replicated after smooth inversion with the D_{rms} converging to a very low level of about 3% after three iterations.

Fig. 12. Sketch map showing the location of study area in northern Germany.

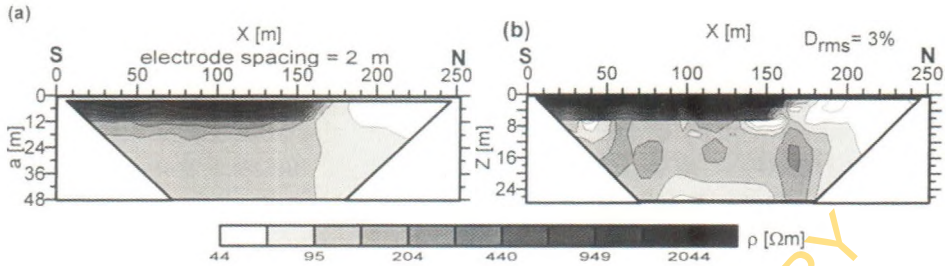

In order to better understand the subtle changes in the resistivity, vertical sets of pseudosection data were examined at different points along the imaging line and treated as electrical soundings and a 1D interpretation of the pseudo-soundings was then carried out. At a distance X = 60 m, a poor fit to the data was obtained when a 2-layer model was employed in fitting the data (Fig. 14a), with the D_{rms} being high at about 6%. This necessitated increasing the number of layers to 3. In this way, an improved fit to the pseudosection data was derived (Fig. 14b), with the D_{rms} being reduced by half. On the other hand, a 2-layer model gave a very good fit to the vertical set of pseudosection data at a distance of X = 190 m along the line (Fig. 15), with the D_{rms} being very low at about 2%.

The foregoing suggests that while a 3-layer model would be required to interpret the data towards the southern part of the line, a 2-layer case would suffice for the northern section. A resistivity of 100 Ωm was assigned to the half-space. Towards the south, the two overburden units were assigned resistivities of 3000 and 500 Ωm, respectively. On the other hand, the single overburden unit towards the north was assigned a resistivity of 40 Ωm The inversion results with the sharp-boundary inversion algorithm are presented in Fig. 16. The D_{rms} converged to between 10 and 11% after about 4 to 6 iterations in all the models calculated. The model resistivity of the high resistivity material varies between about 4050 and 4700 Ωm. That of the intermediate layer varies within a much larger interval at between 135 and 479 Ωm. On the other hand, the model resistivity of the bedrock is well constrained, ranging between about 80 and 100 Ωm. The same applies to the low resistivity surface material towards the north whose model resistivity varies between about 20 and 35 Ωm. It may be pointed out that it was very difficult to interpret the entire pseudosection data with a simple 2-layer model in the block inversion; the D_{rms} converged to a very high level at about 31%, this indicating a poor fit. The interpretation of the electrical imaging data presented here is in good agreement with the information provided by the geo-radar section (Fig. 17).

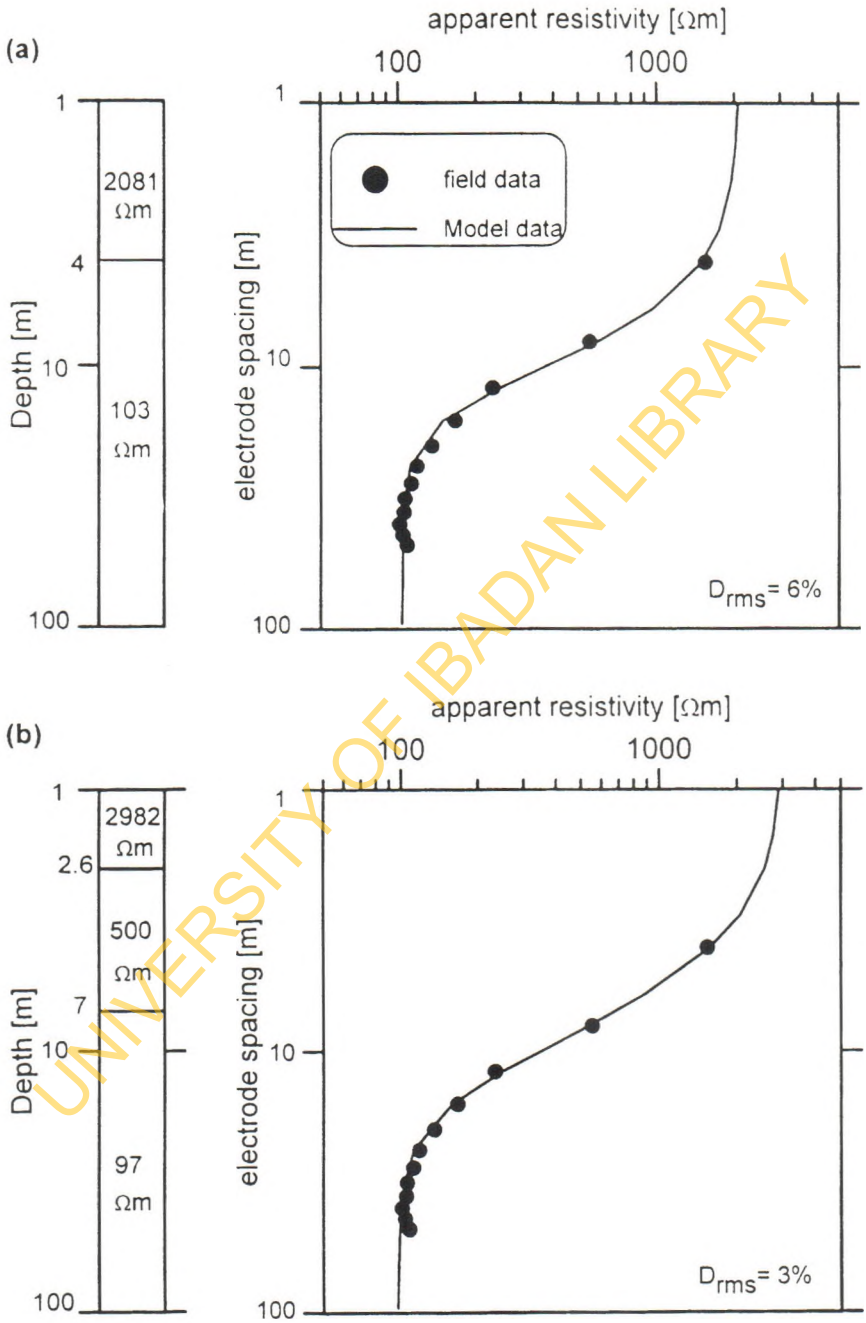

Fig. 14. 1D interpretation of vertical set of pseudosection data at distance X = 60 m along the electrical imaging line. (a) 2-layer model with a data rms misfit of 6%. (b) 3-layer model with a data rms misfit of 2%.

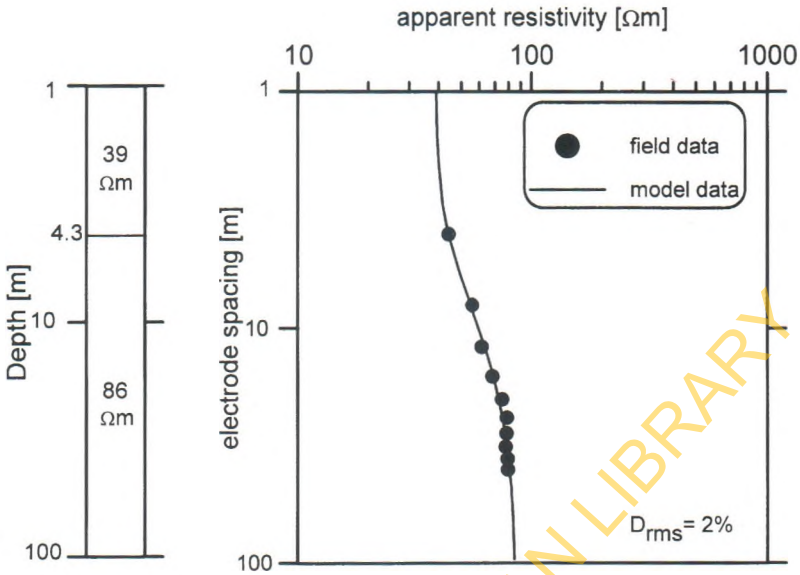

Fig. 15. 1D interpretation of vertical set of pseudosection data at distance X = 190 m along the electrical imaging line with a data rms misfit of 2%.

DISCUSSION AND CONCLUSIONS

Using synthetic data for the Wenner array over simple geologic models in which the substratum is less resistive than the overburden, it is shown in this paper that there is generally an improvement in the model misfit with iteration number in smooth inversion; the algorithm can then be expected to iterate to the best solution at a high iteration number where the model resistivity of the substratum approaches the true bedrock resistivity. In comparison, in cases where there is an increase in resistivity with depth, the model misfit might diverge for successive iterations (Olayinka and Yaramanci, 2000a).

The program used for the block inversion in this work requires that the interpreter prescribes an initial geological model as part of the input. It is demonstrated that such a starting model could be based on a plane layer earth model. This simple approach has the added advantage that only the depth to the interface(s) need be varied as the inversion result is, for all practical purposes, not dependent on the resistivity contrast in the starting model. As the depth to interface in the starting model is increased, it is shown that, contrary to what would be expected intuitively, there is no smooth progression in the inverted model. In other words, it is possible to obtain a reasonable interpretation for both shallow and large depths to the bedrock interface in the starting model.

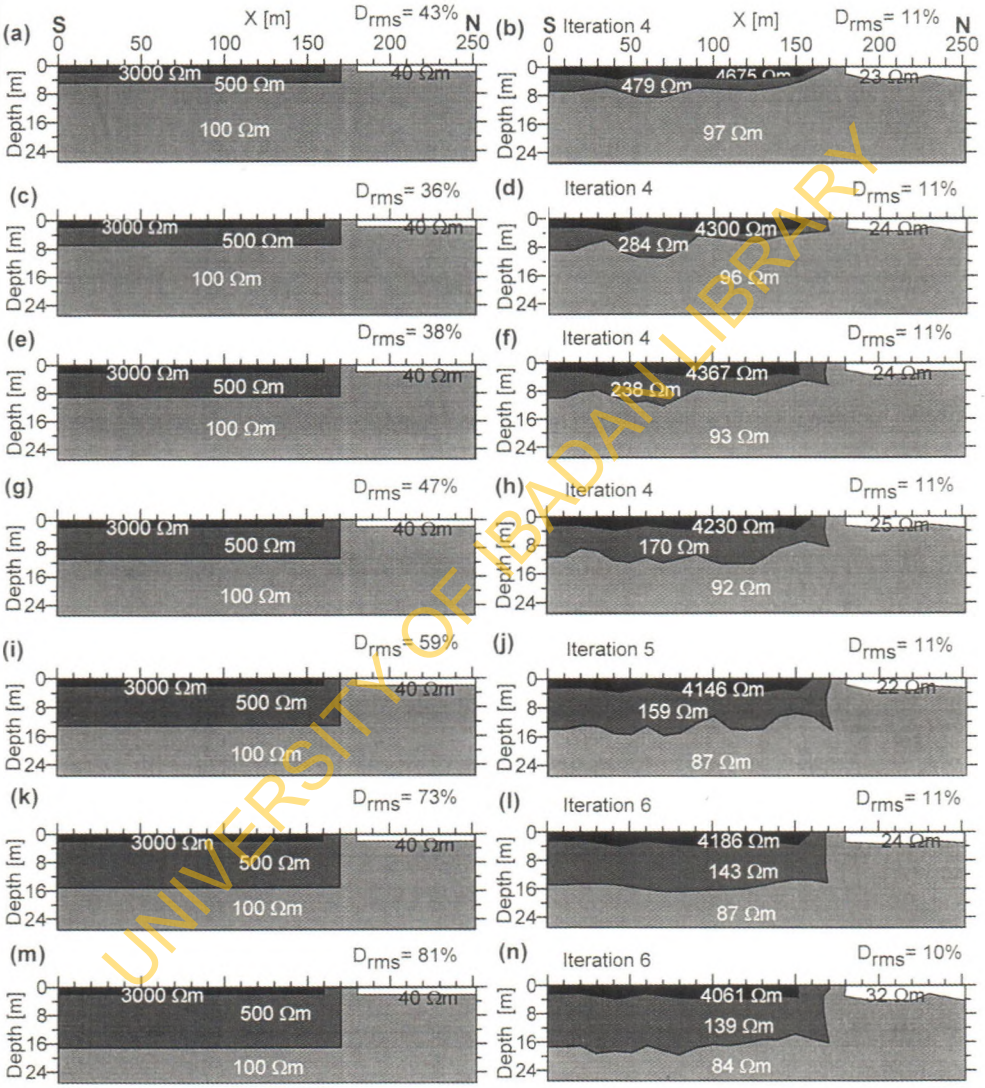

Fig. 16. Model obtained from the sharp-boundary inversion of the measured pseudosection data. The left-hand panels are the initial model prescribed by the interpreter while the right-hand panels are the corresponding inverted 2D models. Note that the data rms misfit stays practically the same in all the equivalent model interpretations.

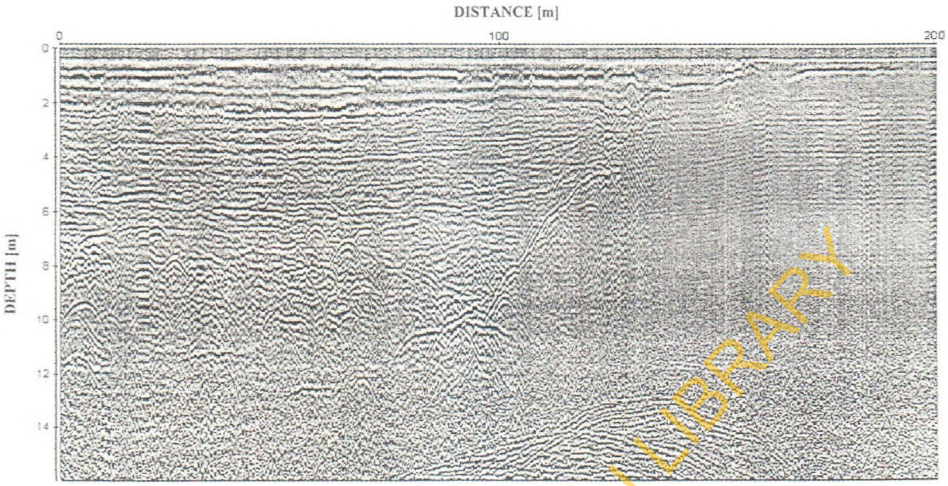

Fig. 17. Geo-radar section from the same traverse as the electrical image line.

Inversion of the data using sharp boundaries indicates that the range of 2D equivalence is relatively narrow, with the data rms misfit being very diagnostic in deciding on a reasonable interpretation. There is often a linear relationship between the data rms misfit and the error in estimating the resistivities in the true model; the data misfit thus provides a straightforward way of identifying the equivalent solutions from the inverted models.

The convergence criterion used in the block inversion was the change in the data rms error such that the inversion process is terminated when the difference between the rms error between two successive iterations is less than 3%. In this way, the inversion could converge after a few iterations to a very high value with a poor fit to the field data. In such cases, the inversion model would be a poor approximation to the field data. On the other hand, convergence might be achieved after several iterations, with a reasonable interpretation obtained.

A field example from Nauen, northern Germany, is presented. In the study area, highly resistive, partly saturated sand in the vadose zone ($\rho \cong 4000$ Ωm), is underlain by less resistive saturated sand ($\rho \cong 150$ Ωm). This, in turn, is underlain by glacial till ($\rho \cong 100$ Ωm). The smooth and sharp-boundary inversion results are in good agreement with the geo-radar, SNMR and borehole information.

ACKNOWLEDGEMENTS

This research was carried out at the Department of Applied Geophysics, Technical University, Berlin, Germany. It was funded through a Research Fellowship awarded to A.I.O. by the Alexander von Humboldt Foundation, Bonn. The authors are grateful to Pietro Cosentino and an anonymous reviewer of this journal for their comments which have assisted in improving the clarity of the paper.

REFERENCES

Dahlin, T.and Loke, M.H., 1998. Resolution of 2D Wenner resistivity imaging as assessed by numerical modelling. J. Appl. Geophys., 38: 237-249.

DeGroot-Hedlin, C. and Constable, C., 1990. Occam's inversion to generate smooth two-dimensional models from magnetotelluric data. Geophysics, 55: 1613-1624.

Ellis, R.G. and Oldenburg, D.W., 1994. The pole-pole 3D DC resistivity inverse problem: a conjugate-gradient approach. Geophys. J. Internat., 119: 187-194.

Inman, J.R., 1985. Resistivity inversion with ridge regression. Geophysics, 50: 2112-2131.

Interpex Limited, 1996. RESIX IP2DI v3, Resistivity and induced polarization data interpretation software. Interpex Limited, Golden, Colorado.

Loke, M.H. and Barker, R.D., 1996. Rapid least-squares inversion of apparent resistivity pseudosections by a quasi-Newton method. Geophys. Prosp., 44: 131-152.

Marquardt, D.W., 1963. An algorithm for least-squares estimation of non-linear parameters. J. Soc. Industr. Appl. Mathem., 11: 431-441.

Olayinka, A.I. and Yaramanci, U., 1999. Choice of the best model in 2D geoelectrical imaging: case study from a waste dump site. Europ. J. Environm. Engin. Geophys., 3: 221-244.

Olayinka, A.I. and Yaramanci, U., 2000a. Assessment of the reliability of 2D inversion of apparent resistivity data. Geophys. Prosp., 48: 293-316.

Olayinka, A.I. and Yaramanci, U., 2000b. Use of block inversion in the 2D interpretation of apparent resistivity data and its comparison with smooth inversion. J. Appl. Geophys., 45: 63-81.

Pelton, W.H., Rijo, L. and Swift, C.M., 1978. Inversion of two-dimensional resistivity and induced-polarisation data. Geophysics, 43: 788-803.

Petrick, W.R., Pelton, W.H. and Ward, S.H., 1977. Ridge regression applied to crustal resistivity sounding data from South Africa. Geophysics, 42: 995-1005.

Rijo, L., 1977. Electromagnetic modelling by the finite element method. PhD thesis, University of Utah, Salt Lake City.

Yaramanci, U., Lange, G. and Hertrich, M., 1999. Surface NMR combined with geoelectrics and radar for aquifer studies in Nauen, Berlin. Extended Abstr., 61st EAGE Conf., Helsinki.